Heliyon 10 (2024) e38792

Contents lists available at ScienceDirect

Heliyon

journal homepage: www.cell.com/heliyon

Research article

Estrogenic post-menopausal anti-osteoporotic mechanism of *Achyranthes aspera* L.: Phytochemicals and network pharmacology approaches

AKM Moyeenul Huq [a], Johnson Stanslas [b], Nisarat Nizhum [c], Md. Nazim Uddin [d], Maulidiani Maulidiani [e], Miah Roney [f], Faridah Abas [g], Jamia Azdina Jamal [a,*]

[a] *Centre for Drug and Herbal Development, Faculty of Pharmacy, Universiti Kebangsaan Malaysia, Jalan Raja Muda Abdul Aziz, 50300, Kuala Lumpur, Malaysia*
[b] *Pharmacotherapeutics Unit, Department of Medicine, Faculty of Medicine and Health Sciences, Universiti Putra Malaysia, 43400, UPM Serdang, Selangor Darul Ehsan, Malaysia*
[c] *Pharmaceutical Research Division, Bangladesh Council of Scientific and Industrial Research, Dhaka, 1205, Bangladesh*
[d] *Institute of Food Science and Technology, Bangladesh Council of Scientific and Industrial Research, Dhaka, 1205, Bangladesh*
[e] *Faculty of Science and Marine Environment, Universiti Malaysia Terengganu, 21030, Kuala Nerus, Terengganu, Malaysia*
[f] *Faculty of Industrial Sciences and Technology, Universiti Malaysia Pahang Al-Sultan Abdullah, Lebuhraya Persiaran Tun Khalil Yaakob, Kuantan, Pahang, Malaysia*
[g] *Laboratory of Natural Products, Institute of Bioscience, Universiti Putra Malaysia, 43400, UPM Serdang, Selangor Darul Ehsan, Malaysia*

ARTICLE INFO

Keywords:
Achyranthes aspera L.
Estrogenic activity
Network pharmacology
Osteoporosis
Phytochemical analysis
Molecular docking

ABSTRACT

Hormone replacement therapy is used to treat postmenopausal syndrome caused by estrogen deficiency, but it has been linked to an increased risk of breast cancer. In India, *Achyranthes aspera* L. is traditionally used to treat menstrual problems; however, there is a lack of mechanistic evidence of its phytoestrogenicity. Therefore, this study investigated the estrogenic activity of *A. aspera* on estrogen-responsive MCF-7 breast cancer cells. In a cell proliferation assay, the MeOH fraction (100 μg/mL) exhibited the highest proliferation effect (PE) of 138 % ($p < 0.001$) and relative proliferation effect (RPE) of 96.5 %, compared to 17β-estradiol (0.01 μM: 143 % PE, $p < 0.001$; 100 % RPE). The MeOH fraction was shown to upregulate the oestrogen marker genes trefoil factor 1 and progesterone receptor by 20.14–23.94 folds and 10.83–14.83 folds, respectively. Twelve phenolics were identified by LC-MS/MS in the active MeOH fraction, i.e. quinic acid, kaempferol hexoside, kaempferol 3-O-(2″-O-galloyl)-glucoside)-β-D-glucoside, geniposide, 3-O-(6′-O-(9Z,12Z-octadecadienoyl)-β-D-glucopyranosyl)-stigmast-5,22E-dien-3β-ol, kaempferol-3-O-glucoside (astragalin), 3,30-di-O-methylellagic acid isomer, procyanidin, naringin, propapyriogenin A2, (3β,22E,24R)-23-methylergosta-5,7,22-trien-3-ol and 6-prenylapigenin. Through network pharmacology, the potential effects, and mechanisms of these compounds in osteoporosis were revealed. About 55 target genes were linked to osteoporosis. GO and KEGG enrichment suggest regulation of female reproductive hormone related signaling pathways, which are also associated with estrogen dependent osteoporosis. Molecular docking analysis of the compounds revealed potential interactions with hERα receptor for 3-O-(6′-O-(9Z,12Z-octadecadienoyl)-β-D-glucopyranosyl)-stigmast-5,22E-dien-3β-ol and kaempferol-3-O-glucoside (astragalin) (docking scores of −9.3 and −10.1 kcal/mol, respectively) as compared to 17β-estradiol (−9.3 kcal/mol).

* Corresponding author.
E-mail address: jamia@ukm.edu.my (J.A. Jamal).

https://doi.org/10.1016/j.heliyon.2024.e38792
Received 27 May 2024; Received in revised form 26 September 2024; Accepted 30 September 2024
Available online 2 October 2024

These results suggest the estrogenicity of *A. aspera* via an ERα-associated mechanism and support its traditional usage in the management of menopausal-related problems.

1. Introduction

Postmenopausal symptoms caused by estrogen deficiency include hot flashes, mood swings, sweating, metabolic syndrome, cognitive impairments, cardiovascular disease, and osteoporosis [1]. Additionally, irregular estrogen hormone levels may increase the risk of breast cancer development [2]. Hormone replacement therapy (HRT) using estrogen, progesterone, or their combination has been the treatment of choice to alleviate such symptoms [3]. However, the Women's Health Initiative (WHI) trials indicated that HRT increases the risk of cardiovascular disease, breast cancer, and stroke [4]. This study led many women to seek natural remedies as alternatives. As a result, researchers have shown significant interest in plant-based substances known as phytoestrogens. Phytoestrogens mimic the function of endogenous estrogen and may have structural similarities. These estrogenic compounds from plants have the ability to bind to estrogen receptors and regulate estrogen signaling pathways [5].

In Asia and the Indian subcontinent, plant-based traditional medicines have been utilized for a variety of women's health issues, such as irregular menstruation, pregnancy, childbirth, lactation, and menopause. For example, the root, leaf, and stem of *Achyranthes aspera* L. (Amaranthaceae) are used in India to treat amenorrhea and dysmenorrhea, as well as to facilitate childbirth [6,7]. The herb is also used to treat ringworm, head wounds, and tonsillitis in East Africa [8]. It has been reported that *A. aspera* contains organic acids, aliphatic hydrocarbons, polysaccharides, pentacyclic triterpenoids, oleanane-type triterpenoid saponins, ketosteroids, steroid glycosides, and polypeptides [9]. Its pharmacological properties include antioxidant, antibacterial, analgesic, anti-inflammatory, spermicidal, wound-healing, and immunomodulatory effects [10]. Recent studies have also revealed that *A. aspera* exhibits strong cerebroprotective effects in rats and can alleviate stress-mediated depression in mice [11,12]. Despite its potential therapeutic activity, the toxic effects of *A. aspera* are a major cause for concern. When administered at a dose of 1000 mg/kg, there is evidence of negative impacts on rat embryonic development and the fetus [13].

Estrogen is recognized as a principal regulator of MCF7 cell proliferation, as evidenced by a breadth of studies. In particular, 17β-estradiol, a highly active form of estrogen, has been shown to significantly boost both the proliferation and migration of breast cancer cells. Empirical findings indicate that 17β-estradiol induces a 24 % increase in MCF7 cell proliferation and enhances cell viability by 36 %. Furthermore, it facilitates cell cycle progression, notably by increasing the G2/M phase population, a critical phase for cell division (Nunes et al., 2017; Tian et al., 2018) [14,15]). The MCF-7 human breast cancer cell line, characterized by its expression of estrogen receptors, exhibits a marked increase in growth rate upon exposure to estrogens, and conversely, a decrease in growth rate in response to antiestrogens (Lykkesfeldt and Sorensen, 1992) [16].

Studies on the mechanism and estrogen-like activities of its traditional application in gynaecological problems and potential effect on one of the major postmenopausal complications like osteoporosis are still missing. Thus, the aim of this study was to evaluate *in vitro* estrogenic activity of *A. aspera* in estrogen-responsive MCF-7 breast cancer cell line and molecular docking considering its potential mechanism in estrogen deficient osteoporosis by integrated network pharmacology approach.

2. Materials and methods

2.1. Plant collection and preparation of A. aspera fractions

Achyranthes aspera whole plants were collected from the Dhaka District of Bangladesh (geographical location coordinate 23.8223° N, 90.3654° E) and identified by Professor Dr. Shaikh Bokhtear Uddin from the Department of Botany, University of Chittagong, Chittagong, Bangladesh. The voucher specimen was deposited at the Chittagong University Herbarium with a reference number MA 24231 CUH. The air-dried plants were ground into a powder and sequentially macerated at room temperature for at least 48 h each with n-hexane, dichloromethane, and methanol. The respective organic fractions were evaporated to dryness using a rotary evaporator. Finally, the aqueous fraction was then prepared by reflux extraction for 2 h and the filtrate was freeze-dried.

2.2. E2 dependent MCF-7 cell proliferation assay

MCF-7 cells (ATCC, USA) were grown in RPMI 1640 medium (Gibco, USA) supplemented with 10%v/v foetal bovine serum (FBS) (Gibco, USA) at 37 °C, 80 % relative humidity and 5 % CO_2. Six days prior to the assay, the cells were subcultured in phenol red-free RPMI with 5%v/v charcoal stripped FBS (Sigma Chemicals Company, USA) and seeded at 5000 cells per well on flat-bottomed 96-well microtitre plates. The next day, test fractions (0.01–100 μg/mL) and the positive control, 17β-estradiol (E2; 0.01 μM), were added to each well, followed by six days of incubation. Then, 3-(4, 5-dimethylthiazol-2-yl)-2,5-diphenyl tetrazolium (MTT) solution was added and then replaced with DMSO before spectrophotometric measurement of absorbance at a wavelength of 550 nm (A_{550}) using a Versamax microplate reader (Molecular Devices, USA). The relative proliferative effect (RPE) was calculated using the following formula:

$$\text{Relative Proliferative Effect } (\%) = \frac{(\text{Proliferative effect of test fraction} - 1)}{(\text{Proliferative effect of } 17\beta - \text{estradiol} - 1)} \times 100$$

2.3. LC-MS/MS analysis of MeOH fraction of A. aspera

Chromatographic separation of the MeOH fraction was done using an AB Sciex 3200QTrap LC-MS/MS with a Flexar FX-15 series UHPLC and a Phenomenex synergi fusion (100 mm 2.1 mm; particle size, 3 μm) to profile the secondary metabolites of the fraction. The eluents used were (A) 1 % formic acid in water and 5 mM ammonium formate, and (B) MeOH with 1 % formic acid and 5 mM ammonium formate. At a flow rate of 250 μL/min, a gradient programme of 10 % A for 5 min, 10–100 % B over 10 min, and 100 % B for 5 min was employed. A negative ionization mode with 500 °C temperature, 4500 V capillary voltage (IS), 100–1500 *m/z* for full scan and 50–1500 *m/z* for MS/MS scan was used. Data was acquired using the ACD/Labs advanced chemometrics mass fragmentations prediction software (Toronto, Canada), and the chromatogram peaks were identified by comparing them to the mass spectral library.

2.4. Network pharmacology study

2.4.1. Target prediction and osteoporosis-associated gene identification

On the basis of network pharmacology-based prediction, We used SwissTargetPrediction tools to performs a combination of similarity measurements based on known 2D and 3D chemical structures to predict the corresponding potential bioactive targets (probability> 0.1, http://www.swisstargetprediction.ch/) [17]. Then we used DisGeNET tool (https://www.disgenet.org/home/) for identifying the osteoporosis –associated genes. Finally, we employed "Calculate and draw custom Venn diagrams" tool to identify the common genes between targeted genes and osteoporosis-associated genes.

2.4.2. Gene ontology (GO) and Kyoto Encyclopedia of genes and genomes (KEGG) pathway enrichment analyses of the target proteins

To identify the role of target proteins that interact with the active ingredients in gene function and signaling pathway, the Database for Annotation, Visualization and Integrated Discovery (DAVID, https://david.ncifcrf.gov/) v6.8 was employed [18]. The GOs and KEGG [19] pathways significantly associated with the predicted genes were identified. The adjusted P value ≤ 0.05 was considered as significant.

2.4.3. Molecular docking of phytochemical compounds from MeOH fraction of A. aspera

The RCSB Protein Data Bank (PDB ID: 7NDO) [20] was used to obtain the co-crystal structure of hER alpha-raloxifen, a protein-ligand complex of the ligand-binding domain of the human oestrogen receptor alpha (hER) and a selective oestrogen receptor modulator (SERM) raloxifen. The CB-DOCK web server (http://cao.labshare.cn/cb-dock/), which requires a target protein in pdb format and ligands with MOL2, MOL, or SDF format, was used to examine the compounds' docking. The server is a blind docking tool that automatically prepares the protein and ligands and converts into a pdbqt format file and uses the CB-DOCK server's curvature-based cavity identification technique. This method employs AutoDock Vina to perform molecular docking after automatically determining the binding sites, computing the centre and size, and customising the docking box size to the query ligands [21]. In this experiment, the.pdb file for the protein and the MOL file for the ligand were uploaded, and 10 potential coupling cavities were identified. Based on the lowest Vina value obtained, the compound with the lowest binding energy was chosen.

2.4.4. ADMET calculation

Various pharmacokinetic properties (absorption, distribution, metabolism, excretion, and toxicity parameters) of the ligands were predicted using pkCSM online-based computer software [22]. The ADMET parameters of the ligands were mainly analyzed. The SMILES of the ligands were inputted to the software, understanding of the active site or binding mechanism is not required.

2.4.5. Effect of A. aspera MeOH fraction on TFF1 and PGR mRNA expression in MCF-7 cells

MCF-7 cells were exposed to various concentrations (0.01–100 μg/mL) of the *A. aspera* MeOH fraction and 17β-estradiol (0.01 μM) for 24 h. Total RNA was extracted and purified in accordance with the RNeasy mini kit's manufacturer's instructions (Qiagen, Germany). cDNAs were synthesized using the QuantiTect Reverse Transcription kit from 1 μg of purified RNA (Qiagen, Germany). Pre-validated primer assays for human trefoil factor 1 (TFF1) (Cat. No.: QT00209608) and human progesterone (PGR) (Cat. No.: QT01005879) genes were used (QuantiTech primer assay system, Qiagen, Germany). The housekeeping gene used was human GAPDH (Forward-5′-TGCCTCCTGCACCACCAACT-3′and reverse -5′-GCCTGCTTCACCACCTTC-3′) (Integrated DNA Technologies, Singapore). Following the manufacturer's instructions, the PCR experiment was carried out using the QuantiNova SYBER Green real-time RT-PCR kit (Qiagen, Germany) and the BIO-RAD iQ5 Multicolor Real-Time PCR Detection System. mRNA expression was normalised using GAPDH. The comparative threshold cycle (Ct) values were analyzed using BIO-RAD iQ5 software.

2.4.6. Statistical analysis

Data from the bioassay were presented as a mean and a standard deviation (SD). Utilizing the GraphPad Prism 6 program (GraphPad Software, Inc., Jolla. CA, USA), one-way ANOVA with Dunnet post-hoc statistical analysis was carried out. Data with a p-value of 0.05 ($p < 0.05$) were considered as significant.

3. Results

3.1. Estrogen-dependent MCF-7 cell proliferation of A. aspera fractions

Fig. 1 shows that only MeOH fraction significantly increased MCF-7 cell proliferation as compared to the estradiol-free control (100 %) at concentrations of 1 μg/mL (123.8 %, $p < 0.05$), 10 μg/mL (126 %, $p < 0.05$) and 100 μg/mL (137.7 %, $p < 0.001$) with the corresponding RPE values of 85.6 %, 87.2 %, and 96.5 %, respectively (Table 1). The proliferative activity of the positive control 17β-estradiol (0.01 M) was 142.54 % ($p < 0.001$) with 100 % RPE.

3.2. LC-MS/MS analysis of MeOH fraction of A. aspera

LC-MS/MS detected a number of secondary metabolites in the MeOH fraction of *A. aspera* (Fig. 2), however only 12 phytochemical compounds were characterised including quinic acid, kaempferol-*O*-hexoside, kaempferol 3-*O*-(2″-*O*-galloyl)-glucoside)-β-D-glucoside, geniposide, 3-*O*-(6′-*O*-(9*Z*,12*Z*-octadecadienoyl)-β-D-glucopyranosyl)-stigmast-5,22*E*-dien-3β-ol, kaempferol-3-*O*-glucoside (astragalin), 3,30-di-*O*-methyl ellagic acid isomer, procyanidin, naringin, propapyriogenin A2, (3 β,22E,24R)-23-methylergosta-5,7,22-trien-3-ol and 6-prenylapigenin (Table 2).

3.3. Compounds targeted the osteoporosis-associated genes

We identified the genes targeted by the compounds under investigation. In total, the target compounds interacted with 244 unique genes (Supplementary Table S1). From this set, we identified 55 genes specifically associated with osteoporosis (Fig. 3), which are detailed in Supplementary Table S2. Some of the key osteoporosis-associated genes that interacted with the compounds include ESR1, AR, ESR2, CYP1B1, MMP2, HSD17B1, MMP13, HSD11B2, S1PR2, PTPN11, and CD38. This suggests that the plant extract interacts with these genes, potentially playing a role in the pathogenesis of osteoporosis.

3.4. Compounds targeted osteoporosis-associated genes are related to the enrichment of GO and KEGG pathways

We imputed the 55 genes into the DAVID tool to identify their functional enrichment (Fig. 4). Our analysis revealed significant biological processes, including GO:0001666~response to hypoxia, GO:0048661~positive regulation of smooth muscle cell

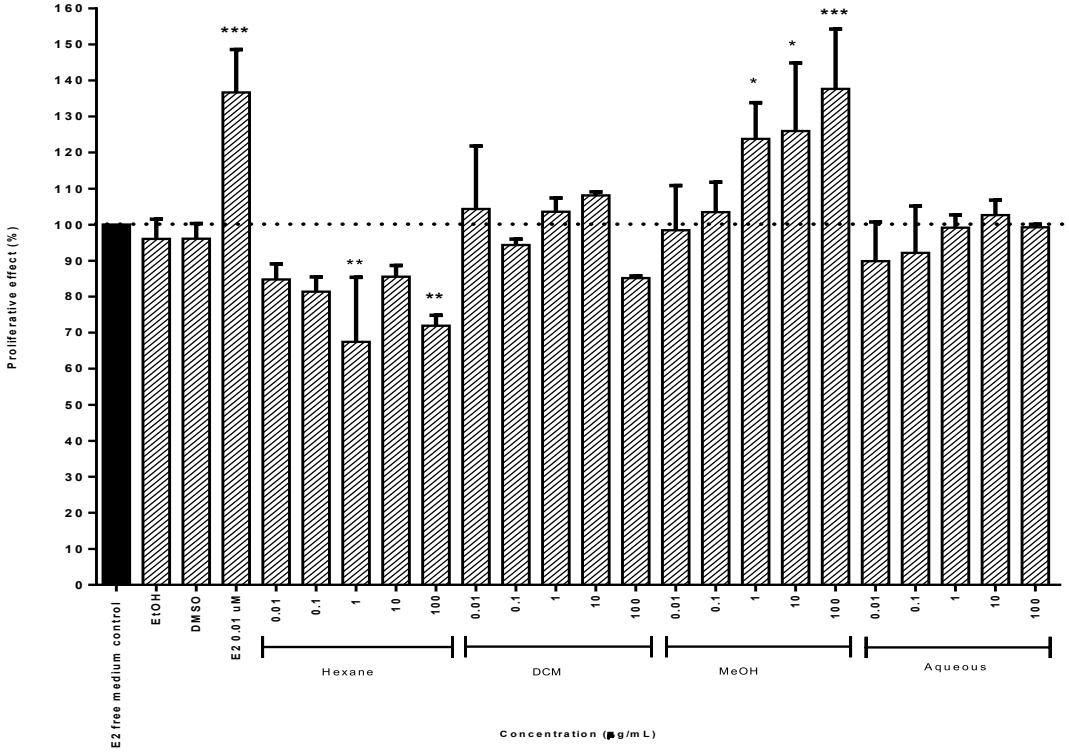

Fig. 1. Effect of *Achyranthes aspera* fractions (0.01–100 μg/mL) on the MCF-7 cell proliferation compared to 17β-estradiol (E2; 0.01 μM) and E2-free control. EtOH and DMSO (0.1 %) were solvent controls. Bars represent mean ± SD of three independent biological replicates (n = 3). Significant difference was calculated by one way ANOVA compared to E2-free medium control with *$p < 0.05$, **$p < 0.01$ and ***$p < 0.001$.

Table 1
Relative proliferative effect (RPE) of MCF-7 cells by *Achyranthes aspera* fractions.

Fractions	Percentage of RPE (%) at different concentrations (μg/mL)				
	0.01	0.1	1	10	100
E2 (μM)	100	–	–	–	–
Hexane	59.15 ± 8.58	56.76 ± 8.21	47.76 ± 15.21	59.61 ± 7.95	50.03 ± 6.84
DCM	89.87 ± 21.82	79.89 ± 7.43	88.21 ± 12.11	91.86 ± 10.53	72.16 ± 8.13
MeOH	68.83 ± 6.92	72.37 ± 4.61	85.64 ± 6.68	87.18 ± 11.78	96.53 ± 9.03
Aqueous	63.57 ± 4.12	65.19 ± 5.28	70.41 ± 0.44	72.89 ± 0.16	70.54 ± 2.05

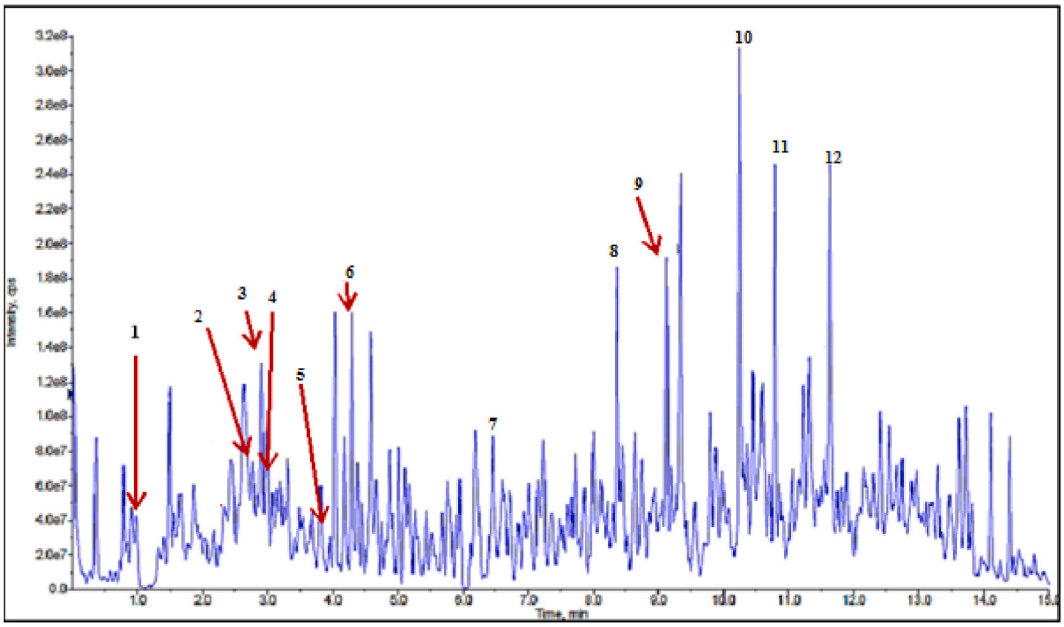

Fig. 2. The UHPLC chromatogram of *Achyranthes aspera* MeOH fraction.

Table 2
Retention time, MS^2 fragments of the compounds present in *A. aspera*.

No.	Tentative compounds identified	Retention time (min)	Molecular ion peak $[M-H]^-$	MS^2 fragmentation ions
1.	Quinic acid	1.399	191	110, 147, 173, 191
2.	Kaempferol-*O*-hexoside	2.906	447	139, 161, 221, 239, 284, 327, 343, 371, 401, 447
3.	Kaempferol 3-*O*-(2″-*O*-galloyl)-glucoside)-β-D-glucoside	2.984	599	137, 285, 299, 313, 505, 599
4.	Geniposide	3.196	388	163, 192, 208, 342, 388
5.	3-*O*-(6′-*O*-(9*Z*,12*Z*-octadecadienoyl)-D-glucopyranosyl)-stigmast-5,22*E*-dien-3β-ol	4.035	835	113, 175, 179, 355, 835
6.	Kaempferol-3-*O*-glucoside (astragalin)	4.293	447	151, 227, 255, 284, 447
7.	3,30-di-O-methylellagic acid isomer	6.603	330	139, 171, 201, 294, 312, 330
8.	Procyanidin	8.371	576	149, 165, 207, 225, 277, 299, 576
9.	Naringin	9.131	580	149, 165, 207, 225, 255, 299, 341, 580
10.	Propapyriogenin A2	10.250	483	153, 171, 227, 245, 255, 302, 483
11.	(3β,22E,24R)-23-methylergosta-5,7,22-trien-3-ol	10.788	409	79, 153, 155, 171, 255, 409
12.	6-Prenylapigenin	11.628	339	119, 170, 239, 276, 339

proliferation, GO:0043406~positive regulation of MAP kinase activity, GO:0009410~response to xenobiotic stimulus, GO:0022900~electron transport chain, GO:0045907~positive regulation of vasoconstriction, GO:0030518~intracellular steroid hormone receptor signaling pathway, GO:0045893~positive regulation of transcription, DNA-templated, GO:0071392~cellular response to estradiol stimulus, and GO:1902895~positive regulation of pri-miRNA transcription from RNA polymerase II promoter (Supplementary Table S3).

Additionally, we identified 18 significant cellular components, including GO:0070062~extracellular exosome,

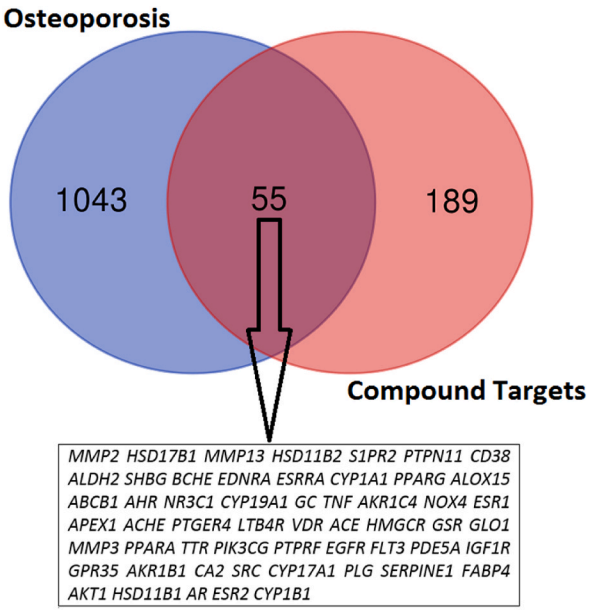

Fig. 3. Identification of 55 genes that are associated with osteoporosis and interacted with compounds.

GO:0005886~plasma membrane, GO:0032991~macromolecular complex, GO:0005615~extracellular space, GO:0043235~receptor complex, GO:0005739~mitochondrion, GO:0000785~chromatin, and GO:0005789~endoplasmic reticulum membrane (Supplementary Table S4).

Furthermore, we identified several key molecular functions, such as GO:0005496~steroid binding, GO:0004879~RNA polymerase II transcription factor activity, ligand-activated sequence-specific DNA binding, GO:0008270~zinc ion binding, GO:0019899~enzyme binding, GO:0009055~electron carrier activity, GO:0003707~steroid hormone receptor activity, GO:0043565~sequence-specific DNA binding, GO:0016491~oxidoreductase activity, GO:0020037~heme binding, and GO:0004175~endopeptidase activity (Supplementary Tables S5A, S5B, and S5C).

Moreover, we identified the KEGG pathways that are associated with these genes. We revealed that the identified genes are associated with the enrichment of estrogenic pathways, such as steroid hormone biosynthesis, ovarian steroidogenesis, endocrine resistance, and estrogen signaling pathway (Table 1). The significant KEGG pathways and their associated genes are tabulated in Table 3. Notably, the *SRC, MMP2, AKT1, ESR1, EGFR, ESR2* genes are involved in the regulation of estrogen signaling pathway (Fig. 5). Altogether, it indicated that the targeted genes are associated with estrogenic signaling in the osteoporosis patients.

3.5. Molecular docking of phytochemical compounds from MeOH fraction of A. aspera

Molecular docking was performed with one of the receptor protein targets involved in the estrogen signaling pathway. The classical or genomic mechanism of estrogen is mediated by the estrogen receptor-alpha (ERα), also known as ESR1. We investigated the binding interactions of 12 phytochemical compounds with the human ERα receptor (hERα/ESR1), as shown in Table 4. Our findings revealed that the endogenous ligand 17β-estradiol binds to chain A of the hERα receptor with a docking score of −9.3 kcal/mol and a cavity size of 2385 Å (Center X, Y, Z: 31, 11, 33). This interaction involved six hydrophobic bonds with LEU346, ALA350, LEU384, GLU353, and LEU391, two hydrogen bonds with PHE404, ARG394, and GLU353, and one pi-pi interaction with PHE404.

The docking scores of the tested phytochemical compounds ranged from −6.1 to −10.1 kcal/mol, with quinic acid showing the lowest Vina score and astragalin the highest. Notably, astragalin demonstrated superior cavity fit and binding, with a docking score of −10.1 kcal/mol—higher than that of 17β-estradiol—despite sharing the same cavity size (2385 Å) and central position (Center X, Y, Z: 31, 11, 33). Astragalin binds exclusively to chain A via 11 amino acid residues, including HIS524, ILE424, MET421, LEU428, LEU391, PHE404, ARG394, GLU353, LEU387, LEU346, and THR347, through 5 hydrophobic interactions, 9 hydrogen bonds, and 1 pi-pi interaction. Astragalin and 17β-estradiol share five common amino acid interactions: LEU391, PHE404, ARG394, GLU353, and LEU346.

Another compound, 3-O-(6′-O-(9Z,12Z-octadecadienoyl)-D-glucopyranosyl)-stigmast-5,22E-dien-3-ol, exhibited the same docking score (−9.3 kcal/mol), cavity size (2385 Å), and central position (Center X, Y, Z: 31, 11, 33) as 17β-estradiol. However, it involved binding amino acids from both chain A (6 residues) and chain B (8 residues), forming 16 hydrophobic bonds and 2 hydrogen bonds. Notably, three amino acids on chain A—ALA350, LEU346, and PHE404—were shared with 17β-estradiol. Despite showing favorable docking scores, the other compounds had minimal bonding similarity to 17β-estradiol in terms of cavity size, central position, and amino acid residue involvement (Table 4).

Fig. 6 illustrates the docking positions of 17β-estradiol, astragalin, and 3-O-(6′-O-(9Z,12Z-octadecadienoyl)-D-glucopyranosyl)-

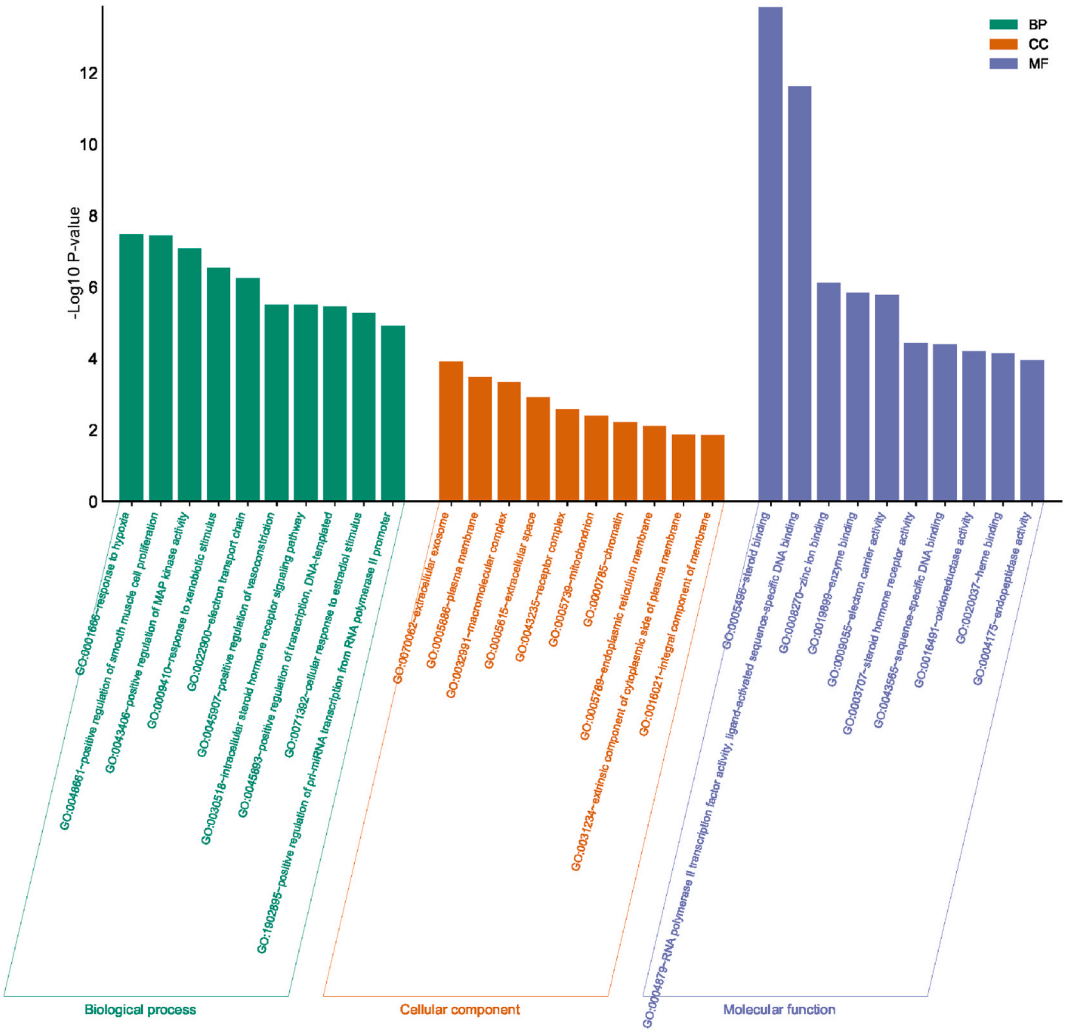

Fig. 4. The top enriched biological processes, cellular components, and molecular functions.

stigmast-5,22E-dien-3-ol with hERα (PDB ID: 7NDO).

3.6. ADMET analysis of identified phytochemicals

The absorption, distribution, metabolism, excretion, and toxicity (ADMET) study can be used to predict the pharmacological properties, metabolizing system, and toxicity of oral drug discovery candidate (Table 5). From the results, all the ligands were expected to be readily absorbed in the human gut, and all exhibited promising logarithm of molar solubility values ranging from −7.25 to −1.67. On the other hand, most of the compounds showed very good absorption (<90.0 %) and the compound 3-*O*-(6′-*O*-(9*Z*,12*Z*-octadecadienoyl)-D-glucopyranosyl)-stigmast-5,22*E*-dien-3β-ol showed the best absorption (96.68 %) in the human intestine.

Moreover, all of the compounds also were anticipated not to have undefined Blood Brain Barrier (BBB). Astragalin, Kaempferol 3-O-(2″-O-galloyl)-glucoside)-β-D-glucoside, Naringin and Quinic acid did not block cytochrome P450, implying that they can easily undergo oxidation and hydroxylation in the initial phase of metabolism [23]. 3-*O*-(6′-*O*-(9*Z*,12*Z*-octadecadienoyl)-D-glucopyranosyl)--stigmast-5,22*E*-dien-3β-ol blocked one cytochrome P450. A potassium ion receptor is produced by the human ether-á-go-go related gene (hERG) that participates in electrical heart activity by repolarizing the cardiac action potential [24]. Inhibiting this channel with drugs might produce an irregular heartbeat (arrhythmia), which can lead to potentially deadly symptoms [25]. According to the prediction, compounds Geniposide, Quinic acid and PropyrogeninA2 tested by the hERG inhibitor predictor had no capacity to block this channel, suggesting their usefulness as a therapeutic option. Rest of the compounds showed the capacity to block hERG II channel.

This programme was also used to predict the hepatotoxicity potential of the ligands. None of the compounds have no hepatoxic profile. So, they were shown to have no risk for liver injury.

Table 3
KEGG pathway and their associated genes.

Term	Count	P Value	Genes
hsa00140:Steroid hormone biosynthesis	8	7.70E-08	*HSD11B1, HSD11B2, HSD17B1, CYP1A1, CYP1B1, AKR1C4, CYP19A1, CYP17A1*
hsa05207:Chemical carcinogenesis - receptor activation	11	4.47E-07	*AR, SRC, VDR, CYP1A1, CYP1B1, AKT1, AHR, PPARA, ESR1, EGFR, ESR2*
hsa04913:Ovarian steroidogenesis	6	1.30E-05	*HSD17B1, CYP1A1, CYP1B1, CYP19A1, CYP17A1, IGF1R*
hsa01522:Endocrine resistance	7	2.59E-05	*SRC, MMP2, AKT1, ESR1, EGFR, ESR2, IGF1R*
hsa05208:Chemical carcinogenesis - reactive oxygen species	9	5.27E-05	*SRC, CYP1A1, CYP1B1, NOX4, AKT1, PTPN11, AHR, AKR1C4, EGFR*
hsa05205:Proteoglycans in cancer	8	2.20E-04	*SRC, MMP2, AKT1, PTPN11, ESR1, TNF, EGFR, IGF1R*
hsa04917:Prolactin signaling pathway	5	8.32E-04	*SRC, AKT1, ESR1, ESR2, CYP17A1*
hsa05200:Pathways in cancer	11	0.001155	*PTGER4, AR, EDNRA, FLT3, MMP2, AKT1, PPARG, ESR1, EGFR, ESR2, IGF1R*
hsa04915:Estrogen signaling pathway	6	0.001444	*SRC, MMP2, AKT1, ESR1, EGFR, ESR2*
hsa05215:Prostate cancer	5	0.002788	*AR, MMP3, AKT1, EGFR, IGF1R*
hsa04933:AGE-RAGE signaling pathway in diabetic complications	5	0.003114	*MMP2, SERPINE1, NOX4, AKT1, TNF*
hsa04931:Insulin resistance	5	0.004106	*AKT1, PTPN11, PPARA, TNF, PTPRF*
hsa04926:Relaxin signaling pathway	5	0.007684	*MMP13, SRC, MMP2, AKT1, EGFR*
hsa04920:Adipocytokine signaling pathway	4	0.008413	*AKT1, PTPN11, PPARA, TNF*
hsa04520:Adherens junction	4	0.0091	*SRC, PTPRF, EGFR, IGF1R*
hsa05417:Lipid and atherosclerosis	6	0.009589	*SRC, MMP3, CYP1A1, AKT1, PPARG, TNF*
hsa04936:Alcoholic liver disease	5	0.010696	*ALDH2, NOX4, AKT1, PPARA, TNF*
hsa05224:Breast cancer	5	0.012033	*AKT1, ESR1, EGFR, ESR2, IGF1R*
hsa01521:EGFR tyrosine kinase inhibitor resistance	4	0.01217	*SRC, AKT1, EGFR, IGF1R*
hsa01100:Metabolic pathways	17	0.017459	*GLO1, ALOX15, GSR, AKR1B1, HMGCR, AKR1C4, CYP19A1, PIK3CG, CYP17A1, HSD11B1, HSD11B2, ALDH2, CA2, HSD17B1, CYP1A1, CD38, PDE5A*
hsa04080:Neuroactive ligand-receptor interaction	7	0.0232	*PTGER4, EDNRA, GPR35, PLG, S1PR2, NR3C1, LTB4R*
hsa05142:Chagas disease	4	0.023976	*ACE, SERPINE1, AKT1, TNF*
hsa04625:C-type lectin receptor signaling pathway	4	0.025215	*SRC, AKT1, PTPN11, TNF*
hsa05219:Bladder cancer	3	0.025656	*SRC, MMP2, EGFR*
hsa00380:Tryptophan metabolism	3	0.026835	*ALDH2, CYP1A1, CYP1B1*
hsa04066:HIF-1 signaling pathway	4	0.028462	*SERPINE1, AKT1, EGFR, IGF1R*
hsa05415:Diabetic cardiomyopathy	5	0.034571	*ACE, MMP2, GSR, AKT1, PPARA*
hsa04152:AMPK signaling pathway	4	0.037123	*AKT1, PPARG, HMGCR, IGF1R*
hsa05163:Human cytomegalovirus infection	5	0.047511	*PTGER4, SRC, AKT1, TNF, EGFR*

3.7. Regulation of estrogenic marker TFF1 and PGR genes

In comparison to the estradiol-free control, the MeOH fraction and 17β-estradiol significantly increased the expression of both TFF1 and PGR genes. The MeOH fraction at concentrations of 0.1–100 μg/mL showed a significant fold change in TFF1 mRNA level of 20.14–23.94 folds ($p < 0.01$) compared to 17β-estradiol (0.001 μM) with 33.08 folds ($p < 0.0001$) (Fig. 7A). Additionally, the MeOH fraction significantly expressed PGR mRNA level of 10.83–14.84 folds ($p < 0.05$), compared to 17β-estradiol (0.01 μM) with 20.36 folds ($p < 0.0001$) (Fig. 7B).

4. Discussion

Estrogen and estrogen-like substances bind to the estrogen receptor (ER) subtypes, ERα and ERβ. MCF-7 cells are ER-positive and express ERα predominately, which stimulates cell proliferation [26]. The MCF-7 cell model is widely employed for evaluating estrogenic activity. Estrogen-dependent cell proliferation is a common, reliable, and efficient approach for evaluating the physiological activity of estrogen or estrogen-like substances. At doses of 1 and 10 μg/mL, the aerial part of *Agrimonia pilosa* exhibited estrogenic activity through the proliferation of MCF-7 cells [1]. Jamal et al. observed a similar outcome for the aqueous extract of *Marantodes ramentaceae* leaves at a concentration of 10^{-5} g/mL [27]. Ligands form complexes with ERα that promote cellular growth. In this investigation, *A. aspera* also exhibited estrogen-like cell proliferation.

The phytochemical composition of the active methanol fraction can be attributed to the estrogenic potential of *A. aspera*. The estrogenic activity of polyphenolic compounds such as ellagic acid, flavonoids or their derivatives such as apigenin and kaempferol, and sterols such as β-sitosterol has been documented [28,29]. Among the compounds, naringin was found to be estrogenic in a cell proliferation assay and to have a better binding relationship with ERβ than ERα in molecular docking [30]. Although there are no reports on 6-prenylapigenin's estrogenic activity, its isomer 8-prenylapigenin has been reported as an ERβ agonist [31]. Kaempferol-3-*O*-glucoside (astragalin) and geniposide identified in the methanol fraction of *A. aspera* were previously isolated from *Achyranthes bidentata* [32,33] from the same genus.

Menopause causes and accelerates bone loss, which is roughly doubled every 5 years after menopause. Majority of postmenopausal females with osteoporosis have bone loss caused by a lack of oestrogen. Rapid bone loss is caused by an increase in bone turnover,

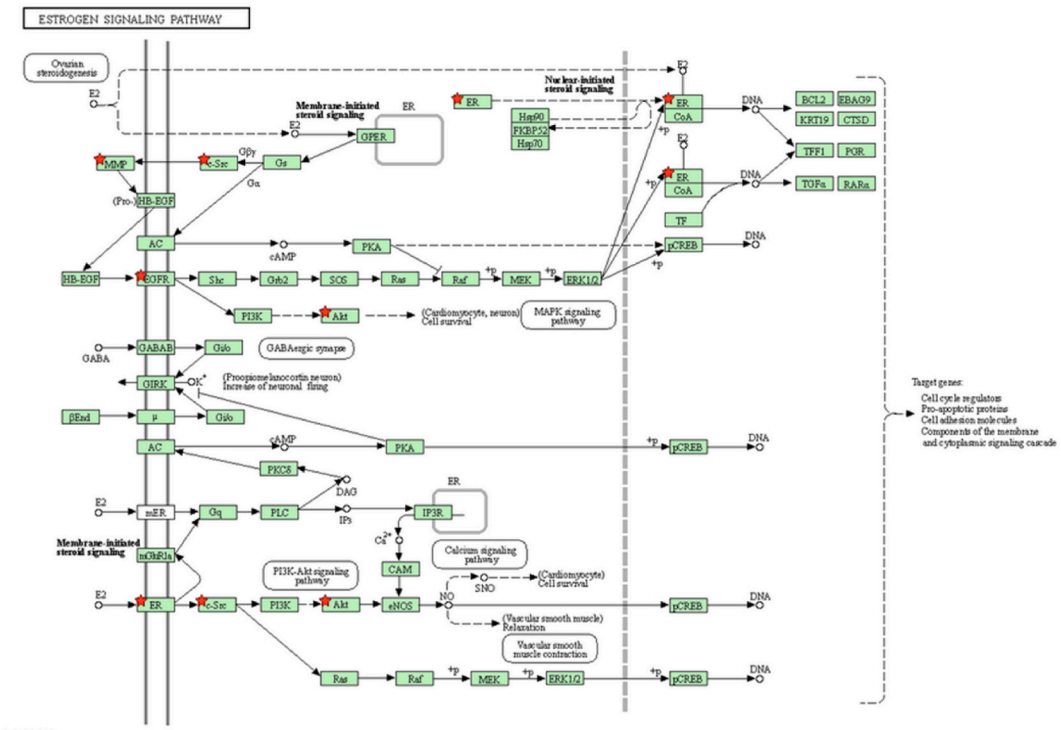

Fig. 5. The *SRC, MMP2, AKT1, ESR1, EGFR, ESR2* genes are involved in the regulation of estrogen signaling pathway.

resulting in an imbalance between bone resorption and bone formation [34,35]. With the rapid development of computer technology and system biology theory, network pharmacology, an emerging interdisciplinary subject, has great advantages to decipher the pharmacologic mechanisms of plant constituents with multi-components, multi-targets, and multi-pathways. The osteoporosis-related targets of the discovered phytochemicals of *A. aspera* were identified in order to investigate the estrogenic mechanism of this plant and its possible pathways oestrogen dependent osteoporosis. According to our study, the chemicals may have an effect on important targets such ESR1, AR, ESR2, CYP1B1, MMP2, HSD17B1, MMP13, HSD11B2, S1PR2, and CD38. These genes modulate biological processes such the intracellular steroid hormone receptor signalling pathway, cellular response to estrogen stimulation, positive regulation on smooth muscle cell proliferation, and MAP kinase activity. Estrogen effects activation of MAPK. *In vivo*, estrogen-induced of MAPK and PI3K signalling activation leading to mitogenesis in MCF-7 cells [36]. Previous studies suggests that the ERK-MAPK pathway can positively regulate bone development [37,38] while the p38-MAPK pathway is vital for bone formation and homeostasis [39]. In the process of osteoclast formation, MAPK signalling pathway regulates downstream factors like c-FOS and NFATc1plays an important part in osteoclast differentiation [40,41].

Endogenous estrogen is involved in the functional processes of both osteoclasts and osteoblasts and maintains haemostasis between them. It also helps in osteogenesis by influencing the proliferation and differentiation of mesenchymal stem cells. Estrogen deficiency hampers the haemostasis in osteoclast levels and the process of osteogenesis, which further can cause osteoporosis [42,43]. Herbal therapy can improve post-menopausal osteoporosis as they contain phytoestrogens. Functionally, these phytoestrogens mimic estrogen like action and influence bone metabolism [44]. Our network pharmacology results suggest that ESR1 and AR are among the major estrogen associated targets of *A. aspera* phytochemicals. Therefore, *A. aspera* may exert beneficial effect in postmenopausal osteoporosis through the estrogen signalling pathway. In a similar study, *Peperomia pellucida* (L.) Kunth which is used to treat osteoporosis was reported to have estrogenic activity [45].

Moreover, steroid hormone receptors essentially mediate the action of several compounds known to affect bone homeostasis such as vitamin D, estrogen and glucocorticoids. We also identified the molecular functions, such as steroid binding and steroid hormone receptor activity by *A. aspera* compounds in this study.

Molecular docking enables the discovery of novel compounds with therapeutic potential and the comprehension of their mechanism of action by anticipating ligand-target interactions at the molecular level by analysing the conformation and alignment of molecules within the binding pocket of the target proteins (often referred to as the "pose"). In this study, the CB-DOCK online tool was utilized, which automatically detects the ligand site, calculates the centre of the binding cavity and its size, and then customizes the docking box based on the query ligands or compounds. The cavity detection or binding site detection uses a surface area model dependent on curvature. The advantage of cavity detection-guided blind docking is that the ligand does not have to bind to the protein's surface, but rather to the putative binding cavities that have been detected. This approach improves the accuracy of ligand docking [46]. In this study, the flavonoid astragalin demonstrated the best docking findings, followed by 3-O-(6′-O(9Z,

Table 4
Docking results of the compounds as identified by LC-MS in *A. aspera* with estrogen receptor alpha (hERα) (PDB ID: 7NDO).

SL	Compound	Vina Score	Cavity size (Å)	Center			Size			Binding residues
				X	Y	Z	X	Y	Z	
1	Estradiol (E2)	−9.3	2385	31	11	33	32	20	20	Chain A: LEU346[a], ALA350[a], LEU384[a], GLU353[a,b], PHE404[b,d], LEU391[a,a], ARG394[b],
2	Quinic acid	−6.1	2296	15	13	14	24	23	26	Chain A: HIS513[c], ARG434[c] Chain B: TYR459[a], HIS476[b], LEU454[b], ASN455[b], ILE475[a]
3	Kaempferol 3-*O*-(2″-*O*-galloyl)-glucoside)-β-D-glucoside	−8.3	2296	15	13	14	24	24	24	ChainA: GLU433[b,b] Chain B: LYS472[b,b], THR460[b,b,b,b], SER468[b], SER463[b], SER464[b]
4	Geniposide	−7.8	2296	15	13	14	21	21	21	Chain B: HIS476[b,b], TYR459[a], LEU378[a], ILE475[a], THR460[b], SER468[b,b,b,b], ASP374[b,b]
5	3-*O*-(6′-*O*-(9*Z*,12*Z*-octadecadienoyl)-D-glucopyranosyl)-stigmast-5,22*E*-dien-3β-ol	−9.3	2385	31	11	33	32	23	23	Chain A: LEU354[a], PRO535[a], ALA350[a], LEU387[a], TRP383[a,a], LEU525[a], LEU346[a], PHE404[a,a] Chain B: ILE475[a], LYS472[a,a], TYR459[a,a], THR460[a,b], SER463[b]
6	Kaempferol-3-*O*-glucoside (astragalin)	−10.1	2385	31	11	33	32	22	22	Chain A: HIS524[b,b], ILE424[a], MET421[b], LEU428[a], LEU391[a,a], PHE404[d], ARG394[b], GLU353[b], LEU387[a], LEU346[b], THR347[b,b,b]
7	3,3-di-O-methylellagic acid isomer	−9.4	2296	15	13	14	20	20	26	Chain B: ARG434[b], HIS476[b], LEU454[b], GLY457[b], TYR459[a], LYS472[a,d], THR460[b,b,b,b,b], ALA430[b]
8	Procyanidin	−8.3	450	35	−1	26	23	23	23	Chain A: TYR526[b,b], GLU380[a,b,b], GLU385[b], ARG515[b], ASN519[b], SER381[a], SER356[a], Chain B: SER381[b], HIS516[b,d], MET427[b], GLU423[a], HIS378[b],
9	Naringin	−8.8	3336	29	−9	4	33	25	25	Chain B: ARG394[b], GLU353[b], LEU391[a], PHE404[a], ALA350[a], LEU387[a], LEU525[a], MET528[b], THR347[b,b,b], ASN532[b,b], ASP351[b], VAL533[b,b], PRO535[b]
10	Propapyriogenin A2	−8.0	450	35	−1	26	23	23	23	Chain B: GLU423[a,b], LYS520[c], HIS516[c] ChainA: SER381[b], MET522[a]
11	3β,22E,24R)-23-methylergosta-5,7,22-trien-3-ol	−9	2296	15	13	14	23	23	23	Chain B: LYS472[a,a,a], THR460[a], ILE475[a], TYR459[a,a], HIS513[b], ASN455[b]
12	6-Prenylapigenin	−9.1	2296	15	13	14	23	23	23	Chain A: HIS513[b], Chain B: ASN455[b], TYR459[a], LYS472[a], ASP374[b], HIS377[b,b]

Note: [a]Hydrophobic bond; [b]Hydrogen bond; [c]Ionic bond, [d]Pi-pi interaction.

12Z-octadecadienoyl)-D-glucopyranosyl)-stigmast-5,22E-dien-3-ol, when compared to the endogenous hormone in terms of docking scores and binding amino acids.

The upregulation of ERα-related genes is associated with the proliferation of estrogen-dependent MCF-7 cells. The expression of endogenous estrogen-regulated genes, such as TFF1 and PGR that are involved in cell proliferation, may be linked to a compound's estrogenic activity. TFF1 and PGR are both used as biomarkers for the response to oestrogen [47,48]. An *in vivo* investigation found that 200 mg/kg of the chloroform and ethanol extracts of *A. aspera* root exhibited estrogenic effect in a uterotropic experiment in rats [49]. In addition, another study showed that *Achyranthes* species, *A. bidentata*, revealed an increase in the expression of ERα, ERβ, and the G-protein coupled estrogen receptor (GPR30) in rat kidney tissue [50]. Moreover, studies also showed that Astragalin helps in bone formation by promoting osteoblastic differentiation [21] and did not exhibit any cytotoxicity up to 400 μg/mL to human fibroblast cell [51]. In this study, the upregulation of these genes by the methanol fraction of *A. aspera* may indicate estrogenic activity via the ERα mechanism.

5. Conclusion

The present study demonstrates the estrogenic activity of the methanol fraction of *A. aspera* through the ERα-mediated expression of the TFF1 and PGR genes, which may be associated with its phytochemical compounds. The extract may also potentially be beneficial in estrogen deficient osteoporosis in postmenopausal women. This provides preliminary evidence for its estrogenic mechanism and traditional use in the treatment of gynaecological problems, such as postmenopausal symptoms. Therefore, additional research is required to elucidate its benefits in *in vitro* and *in vivo* models.

Declaration of generative AI and AI-assisted technologies in the writing process

During the preparation of this work the author(s) used [Quillbot, Grammarly and ChatGpt] in order to [paraphrasing, correcting spelling and grammatical errors and improving the quality of language]. After using this tool/service, the author(s) reviewed and

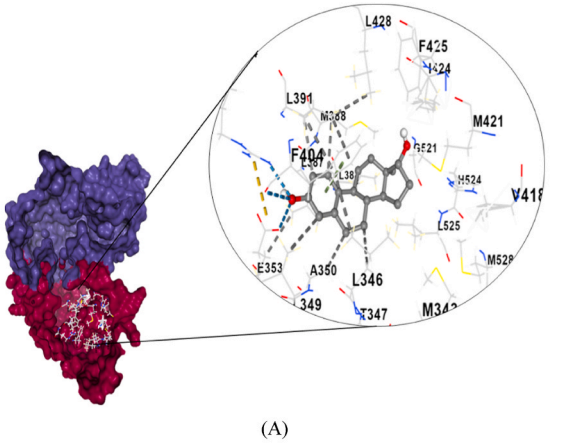

(A)

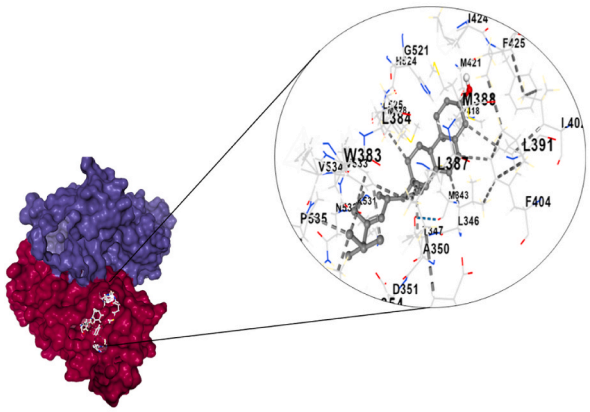

(B)

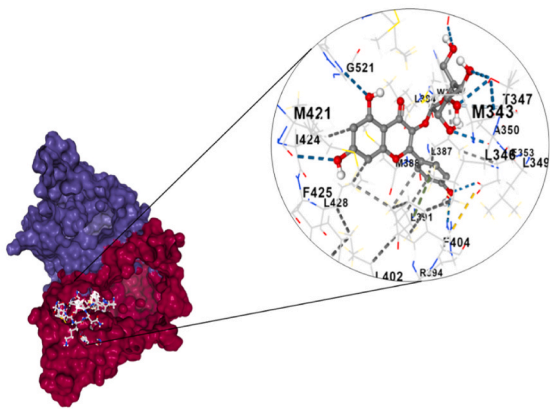

(C)

Fig. 6. Docking interactions of two best fit phytochemicals of *A. aspera* with same binding cavity size as compared to the positive control estradiol. (A) Estradiol, (B) 3-*O*-(6′-*O*-(9*Z*,12*Z*-octadecadienoyl)-D-glucopyranosyl)-stigmast-5,22*E*-dien-3β-ol, and (C) Astragalin with target protein.

edited the content as needed and take(s) full responsibility for the content of the publication. We also declare that the original draft of the manuscript was written by the authors without using any generative AT technology.

CRediT authorship contribution statement

AKM Moyeenul Huq: Investigation, Writing – original draft, Visualization, Methodology, Formal analysis, Data curation. **Johnson**

Table 5
ADMET (absorption, distribution, metabolism, excretion, and toxicity) profile of docked compounds.

C/Name	Absorption		Distribution	Metabolism							Excretion	Toxicity			
	AS	HIA	BBB	Substrates		Inhibitors					Renal OCT2	AMES toxicity	hERG I	hERG II	HT
				CYP2D	CYP3A4	CYP1A2	CYP2C19	CYP2C9	CYP2D6	CYP3A4					
Estradiol (E2)	−4.47	93.41	0.01	No	Yes	Yes	Yes	No	No	No	No	No	No	Yes	No
Quinic acid	−1.67	14.74	−0.99	No	No	No	No	No	No	No	No	No	No	No	No
Kaempferol 3-O-(2″-O-galloyl)-glucoside)-β-D-glucoside	−2.98	30.14	−2.58	No	No	No	No	No	No	No	No	No	No	Yes	No
Geniposide	−2.64	40.44	−1.25	No	No	No	No	No	No	No	No	No	No	No	No
3-*O*-(6′-*O*-(9*Z*,12*Z*-octadecadienoyl)-D-glucopyranosyl)-stigmast-5,22*E*-dien-3β-ol	−7.25	96.68	0.78	No	Yes	No	No	No	No	No	No	No	No	Yes	No
Astragalin	−2.72	35.33	−1.82	No	No	No	No	No	No	No	No	No	No	Yes	No
3,3-di-O-methylellagic acid isomer	−3.98	88.53	−0.40	No	No	Yes	No	No	No	No	No	No	No	No	Yes
Procyanidin	−2.89	48.71	−2.10	No	No	No	No	Yes	No	No	No	No	No	Yes	No
Naringin	−2.43	18.93	−1.81	No	No	No	No	No	No	No	No	No	No	Yes	No
PropyrogeninA2	−4.29	91.50	0.44	No	Yes	No	No	No	No	No	No	No	No	No	No
6-prenylapigenin	−3.85	91.49	−1.00	No	No	Yes	Yes	Yes	No	Yes	No	No	No	Yes	Yes

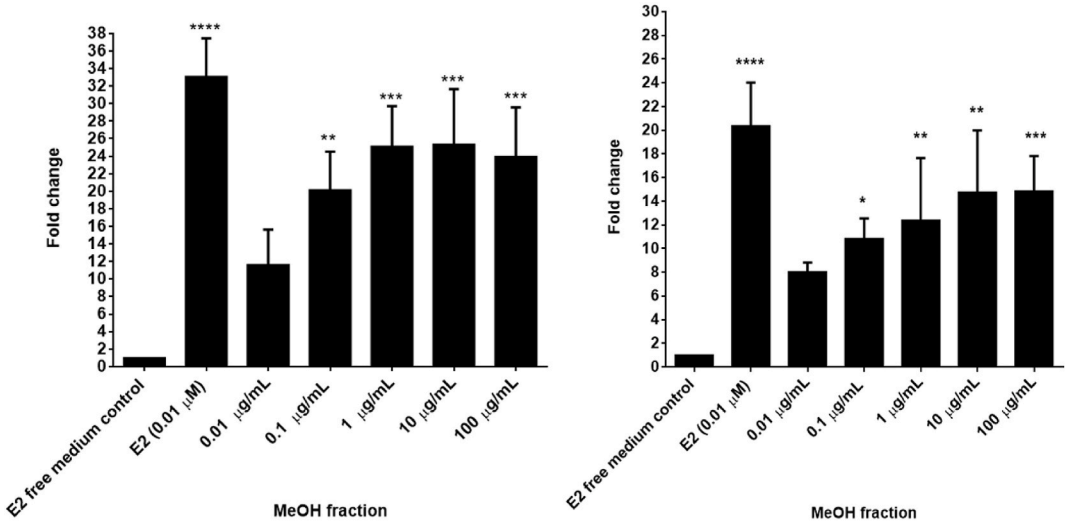

Fig. 7. Level of expression of (a) TFF1 and (b) PGR genes in MCF-7 cells after treatment with 0.01–100 μg/mL of *Achyranthes aspera* MeOH fraction and E2 (0.01 μM). GAPDH reference gene was used to normalize the expression level. Data are represented as mean fold change ± SD of three independent biological replicates (n = 3) (*$p < 0.05$, **$p < 0.01$, ***$p < 0.001$, ****$p < 0.0001$ vs. E2-free medium control).

Stanslas: Supervision, Resources, Writing – review & editing, Visualization, Validation. **Nisarat Nizhum:** Writing – review & editing, Visualization, Formal analysis. **Md. Nazim Uddin:** Writing – original draft, Visualization, Methodology, Formal analysis. **Maulidiani Maulidiani:** Writing – review & editing, Validation, Resources, Investigation, Data curation. **Miah Roney:** Writing – original draft, Visualization, Methodology, Formal analysis. **Faridah Abas:** Writing – review & editing, Resources, Investigation. **Jamia Azdina Jamal:** Writing – review & editing, Validation, Supervision, Resources, Investigation, Funding acquisition, Conceptualization.

Declaration of competing interest

The authors declare that they have no known competing financial interests or personal relationships that could have appeared to influence the work reported in this paper.

Acknowledgements

The authors thank the Ministry of Agriculture, Malaysia for the NKEA research grant scheme funding (NH1014D030).

Appendix A. Supplementary data

Supplementary data to this article can be found online at https://doi.org/10.1016/j.heliyon.2024.e38792.

References

[1] Y.M. Lee, J.B. Kim, J.H. Bae, et al., Estrogen-like activity of aqueous extract from Agrimonia pilosa Ledeb. in MCF-7 cells, BMC Complement Altern Med 12 (2012) 260–268.
[2] D. Germain, Estrogen carcinogenesis in breast cancer, Endocrinol. Metabol. Clin 40 (3) (2011) 473–484.
[3] A.M. Kaunitz, J.E. Manson, Management of menopausal symptoms, Obstet. Gynecol. 126 (4) (2015) 859–876.
[4] J.E. Rossouw, G.L. Anderson, R.L. Prentice, et al., Writing Group for the Women's Health Initiative Investigators. Risks and benefits of estrogen plus progestin in healthy postmenopausal women: principal results from the Women's Health Initiative randomized controlled trial, JAMA 288 (3) (2002) 321–333.
[5] A.V. Sirotkin, A.H. Harrath, Phytoestrogens and their effects, Eur. J. Pharmacol. 15 (741) (2014) 230–236.
[6] A.K. Das, B. Dutta, G. Sharma, Medicinal plants used by different tribes of Cachar district, Assam, Ind J Tradit Know 7 (3) (2008) 446–454.
[7] S. Balamurugan, S. Vijayakumar, S. Prabhu, et al., Traditional plants used for the treatment of gynaecological disorders in Vedaranyam taluk, South India - an ethnomedicinal survey, J Tradit Complement Med 7 (1) (2017) 1–16.
[8] A.R. Ndhlala, H.M. Ghebrehiwot, B. Ncube, et al., Antimicrobial, anthelmintic activities and characterisation of functional phenolic acids of Achyranthes aspera Linn.: a medicinal plant used for the treatment of wounds and ringworm in East Africa, Front. Pharmacol. 6 (2015) 274.
[9] X. He, X. Wang, J. Fang, et al., The genus Achyranthes: a review on traditional uses, phytochemistry, and pharmacological activities, J. Ethnopharmacol. 203 (2017) 260–278.

[10] S. Prakash, A review article on phytochemical and pharmacological profiles of Apamarga (Achyranthes aspera Linn), Int Ayurved Medical J 3 (9) (2015) 2901–2909.
[11] G.L. Viswanatha, M.V. Venkataranganna, N.B.L. Prasad, et al., Achyranthes aspera Linn. alleviates cerebral ischemia-reperfusion-induced neurocognitive, biochemical, morphological and histological alterations in Wistar rats, J. Ethnopharmacol. 10 (228) (2019) 58–69.
[12] D. Gawande, S. Barewar, J. Taksande, et al., Achyranthes aspera ameliorates stress induced depression in mice by regulating neuroinflammatory cytokines, J Tradit Complement Med 12 (6) (2022) 545–555.
[13] D. Teshome, C. Tiruneh, L. Berhanu, et al., Developmental toxicity of ethanolic extracts of leaves of *Achyranthes aspera*, Amaranthaceae in rat embryos and fetuses, J. Exp. Pharmacol. 13 (2021) 555–563.
[14] C. Nunes, C. Silva, A. Correia-Branco, F. Martel, Lack of effect of the procarcinogenic 17Ï^2-estradiol on nutrient uptake by the MCF-7 breast cancer cell line, Biomed. Pharmacother. 90 (2017) 287–294.
[15] J. Tian, B. Ran, Cl Zhang, D. Yan, X. Li, Estrogen and progesterone promote breast cancer cell proliferation by inducing cyclin G1 expression, Braz. J. Med. Biol. Res. 51 (3) (2018) 1–7.
[16] A.E. Lykkesfeldt, E.K. Sørensen, Effect of estrogen and antiestrogens on cell proliferation and synthesis of secreted proteins in the human breast cancer cell line MCF-7 and a tamoxifen resistant variant subline, AL-1, Acta Oncol 31 (2) (1992) 131–138.
[17] D. Gfeller, A. Grosdidier, M. Wirth, et al., SwissTargetPrediction: a web server for target prediction of bioactive small molecules, Nucleic Acids Res. 42 (Web Server issue) (2014) 32–38.
[18] D.W. Huang, B.T. Sherman, R.A. Lempicki, Bioinformatics enrichment tools: paths toward the comprehensive functional analysis of large gene lists, Nucleic Acids Res. 37 (1) (2009) 1–13.
[19] M. Kanehisa, M. Furumichi, M. Tanabe, et al., KEGG: new perspectives on genomes, pathways, diseases and drugs, Nucleic Acids Res. 45 (1) (2017) 353–361.
[20] M. Kriegel, H.J. Wiederanders, S. Alkhashrom, et al., A PROSS-designed extensively mutated estrogen receptor α variant displays enhanced thermal stability while retaining native allosteric regulation and structure, Sci. Rep. 11 (1) (2021) 10509.
[21] L. Liu, D. Wang, Y. Qin, et al., Astragalin promotes osteoblastic differentiation in mc3t3-E1 cells and bone formation in vivo, Front. Endocrinol. 16 (10) (2019) 228.
[22] D. Jain, R. Hossain, R.A. Khan, et al., Computer-aided evaluation of anti-SARS-CoV-2 (3-chymotrypsin-like protease and transmembrane protease serine 2 Inhibitors) activity of cepharanthine: an in silico approach, Biointerface Res Appl Chem 12 (2021) 768–780.
[23] S.F. Zhou, Polymorphism of human cytochrome P450 2D6 and its clinical significance: part II, Clin. Pharmacokinet. 48 (2009) 761–804.
[24] Y.P. Shi, S. Thouta, T.W. Claydon, Modulation of hERG K+ channel deactivation by voltage sensor relaxation, Front. Pharmacol. 11 (2020) 139.
[25] L.X. Cubeddu, Drug-induced inhibition and trafficking disruption of ion channels: pathogenesis of QT abnormalities and drug-induced fatal arrhythmias, Curr. Cardiol. Rev. 12 (2016) 141–154.
[26] D. Kostelac, G. Rechkemmer, K. Briviba, Phytoestrogens modulate binding response of estrogen receptors α and β to the estrogen response element, J Food Agric Chem 51 (26) (2003) 7632–7635.
[27] J.A. Jamal, N. Ramli, J. Stanslas, et al., Oestrogenic activity of selected Myrsinaceae species in MCF-7 human breast cancer cells, Int J Pharm Pharm Sci 4 (2012) 547–553.
[28] Z. Papoutsi, E. Kassi, A. Tsiapara, et al., Evaluation of estrogenic/antiestrogenic activity of ellagic acid via the estrogen receptor subtypes ERα and ERβ, J. Sci. Food Agric. 53 (20) (2015) 7715–7720.
[29] J.C. Kalita, S.R. Milligan, In vitro estrogenic potency of phytoestrogen-glycosides and some plant flavonoids, Ind J Sci Technol 3 (12) (2010) 1142–1147.
[30] L. Sang-Jun, C. Ha-Yull, G.A.M. Camelia, et al., Estrogenic flavonoids from Artemisia vulgaris L, J Food Agric Chem 46 (8) (1998) 3325–3329.
[31] O. Zierau, S. Gester, P. Schwab, et al., Estrogenic activity of the phytoestrogens naringenin, 6-(1,1-dimethylallyl)naringenin and 8-prenylnaringenin, Planta Med. 68 (5) (2002) 449–451.
[32] A. Hajirahimkhan, O. Mbachu, C. Simmler, et al., Estrogen receptor (ER) subtype selectivity identifies 8-prenylapigenin as an ERβ agonist from Glycyrrhiza inflata and highlights the importance of chemical and biological authentication, J Nat Prod 81 (4) (2018) 966–975.
[33] S. Nicolov, N. Thuan, V. Zheljazkov, Flavonoids from Achyranthes bidendata BC, Acta Hortic. 426 (1996) 75–78.
[34] D.L. Meng, Studies of the Constituents and Biological Activities of Achyranthes Bidentata BL, vol. 23, PhD Thesis of Shenyang Pharm Univ, 2004.
[35] E.P. Boschitsch, E. Durchschlag, H.P. Dimai, Age-related prevalence of osteoporosis and fragility fractures: real-world data from an Austrian menopause and osteoporosis clinic, Climacteric 20 (2017) 157–163.
[36] C.H. Cheng, L.R. Chen, K.H. Chen, Osteoporosis due to hormone imbalance: an overview of the effects of estrogen deficiency and glucocorticoid overuse on bone turnover, Int. J. Mol. Sci. 23 (2022) 1376.
[37] E.K. Lobenhofer, G. Huper, J.D. Iglehart, et al., Inhibition of Mitogen-Activated Protein Kinase and Phosphatidylinositol 3-kinase Activity in MCF-7 Cells Prevents Estrogen-Induced Mitogenesis, 2000, pp. 99–110.
[38] C. Ge, G. Xiao, D. Jiang, et al., Critical role of the extracellular signal-regulated kinase-MAPK pathway in osteoblast differentiation and skeletal development, J. Cell Biol. 176 (2007) 709–718.
[39] J.H. Shim, M.B. Greenblatt, W. Zou, et al., Schnurri-3 regulates ERK downstream of WNT signaling in osteoblasts, J. Clin. Invest. 123 (2013) 4010–4022.
[40] S. Weske, M. Vaidya, A. Reese, et al., Targeting sphingosine-1-phosphate lyase as an anabolic therapy for bone loss, Nat Med 24 (2018) 667–678.
[41] S. Liao, W. Feng, Y. Liu, et al., Inhibitory effects of biochanin A on titanium particle-induced osteoclast activation and inflammatory bone resorption via NF-κB and MAPK pathways, J. Cell. Physiol. 236 (2) (2021) 1432–1444.
[42] T. Miyazaki, H. Katagiri, Y. Kanegae, et al., Reciprocal role of ERK and NF kappaB pathways in survival and activation of osteoclasts, J. Cell Biol. 148 (2) (2000) 333–342.
[43] X. Li, Q. Jie, H. Zhang, et al., Disturbed MEK/ERK signaling increases osteoclast activity via the hedgehog-gli pathway in postmenopausal osteoporosis, Prog. Biophys. Mol. Biol. 122 (2) (2016) 101–111.
[44] K. Ikeda, K. Horie-Inoue, S. Inoue, Functions of estrogen and estrogen receptor signaling on skeletal muscle, J. Steroid Biochem. Mol. Biol. 191 (2019) 105375.
[45] Z.C. Thent, S. Das, P. Mahakkanukrauh, et al., Osteoporosis: possible pathways involved and the role of natural phytoestrogens in bone metabolism, Sains Malays. 48 (9) (2019) 2007–2019.
[46] Kartika Igaa, Insanu Muhamad, Riani Catur, et al., Polarity difference and the presence of phytoestrogen compounds affecting estrogenic activity of Peperomia pellucida extracts, Sains Malays. 50 (2) (2021) 449–460.
[47] Y. Cao, L. Li, Improved protein–ligand binding affinity prediction by using a curvature-dependent surface-area model, Bioinformat 30 (12) (2014) 1674–1680.
[48] M. Jørgensen, B. Vendelbo, N.E. Skakkebaek, Assaying estrogenicity by quantitating the expression levels of endogenous estrogen-regulated genes, Environ. Health Perspect. 108 (5) (2000) 403–412.
[49] N. Vasudeva, S.K. Sharma, Estrogenic and pregnancy interceptory effects of *Achyranthes aspera* Linn. root, Afr J Tradit Complement Altern Med 4 (1) (2006) 7–11.
[50] S. Wang, M. Zeng, B. Li, et al., Raw and salt-processed *Achyranthes bidentata* attenuate LPS-induced acute kidney injury by inhibiting ROS and apoptosis via an estrogen-like pathway, Biomed. Pharmacother. 129 (2020) 110403.
[51] M. Ivanov, A. Kannan, D. Stojkovic, et al., Revealing the astragalin mode of anticandidal action, EXCLI J 19 (2020) 1436–1445.